Spectral- and frequency-encoded fluorescence imaging

Jason T. Motz, Dvir Yelin, Benjamin J. Vakoc, and Brett E. Bouma

Harvard Medical School and the Wellman Center for Photomedicine, Massachusetts General Hospital, 55 Fruit Street, BAR 703, Boston, Massachusetts 02114

Guillermo J. Tearney

Harvard Medical School, Wellman Center for Photomedicine and the Pathology Service, Massachusetts General Hospital, 55 Fruit Street, BAR 703, Boston, Massachusetts 02114

Received May 13, 2005; accepted June 13, 2005

A method for obtaining fluorescence images with a high number of resolvable points by using spectral and frequency encoding is presented. Broadband excitation light is encoded with a wavelength-dependent frequency modulation and dispersed onto the sample with a grating to simultaneously illuminate an entire image line. The Fourier transform of the frequency-encoded fluorescence emission provides one line of the image. Mechanical scanning along a direction orthogonal to the wavelength-encoded axis allows creation of the two-dimensional fluorescent image. This method is applicable for developing submillimeter diameter endoscopes. The principles of the technique are validated by imaging indocyanine green fluorescence in microfluidic channels. © 2005 Optical Society of America

OCIS codes: 170.2150, 170.6280, 110.2970, 120.3890.

In vivo fluorescence macroscopic imaging is increasingly being used for clinical disease diagnosis and small animal research. Extending fluorescence imaging to enable a wide range of basic and clinical applications requires the development of flexible, miniaturized endoscopes 1 mm or less in diameter. Two groups have recently reported such devices. Laemmel *et al.*[1] used probes varying in diameter from 600 μm to 1.8 mm to obtain images of vessels in the mouse cremaster muscle and to visualize labeled circulating cells. Images of cells labeled with FITC fluorescein (excitation 488 nm) were acquired at 12 Hz with a maximal field of view of 400 μm$\times$280 μm through probes with ~10,000 optical fibers.[1] Funovics *et al.*[2] developed an 800 μm diameter endoscope with 10,000 optical fibers for use with Cy5.5, excited at 673 nm.[2] The imaging tip, which has a 56° field of view in water, also allows for white-light reflectance imaging with a resolution of 7 line pairs/mm, as determined with a U.S. Air Force 1951 resolution target. Images were presented from mouse vasculature and of protease activity in an ovarian tumor with rates ranging from 3 to 10 Hz.[3] Tumors expressing green fluorescent protein were also observed.[3]

In this Letter we present the principles of an alternative approach, spectral- and frequency-encoded (SFE) fluorescence imaging, which can potentially be performed in a submillimeter diameter endoscope with a high number of resolvable points. Spectral encoding has been previously demonstrated for reflectance imaging.[4,5] In this technique, broadband light from an optical fiber is dispersed by a grating and focused onto a line on the sample, eliminating the need to scan the image in this dimension. Reflected light returns through the lens, grating, and optical fiber, and the spectrally encoded image is then decoded via heterodyne Fourier transform spectroscopy[4] or with another grating in conjunction with a CCD detector.[5] The transverse dimension can then be scanned by, for example, rotating the fiber and distal optics, which is straightforward to implement in small-diameter probes.[6] With this technique, the number of resolvable points (n) along one spectrally encoded line is determined by the spectral bandwidth ($\Delta\lambda$), center wavelength (λ_0), beam diameter (d), and grating:

$$n \cong \frac{\Delta\lambda d G}{\lambda_0 \cos(\theta_i)}, \tag{1}$$

where G and θ_i are the grating groove density and the incidence angle, respectively.[5]

Spectrally encoded fluorescence is based on the same principle, only now the fluorescence emission has been Stokes shifted and the spatial locations are no longer uniquely related to the detected wavelengths. As a result, spectroscopic methods are no longer effective for decoding the image. In order to recapture the spatial information, SFE imaging utilizes a wavelength-dependent frequency modulation of the excitation light before it is dispersed onto the sample via the grating. The fluorescence emission at each location is therefore modulated in concert with the frequency of the excitation light, producing an additional level of encoding. To this end (Fig. 1), broadband excitation light from a $Ti:Al_2O_3$ laser (Femtolasers Produktions, GmbH, Femtosource Integral OCT, center wavelength 800 nm, 150 nm FWHM bandwidth) was passed through an 800 nm shortpass filter (SPF) and directed through a single-mode optical fiber (SMF) into a scanning Michelson interferometer. The scanning interferometer introduced the wavelength-dependent frequency modulation,

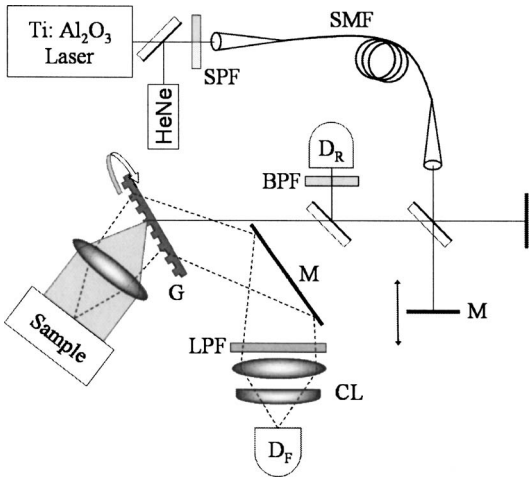

Fig. 1. SFE fluorescence imaging experimental setup: SPF, short-pass filter; SMF, single-mode fiber; M, mirror; BPF, bandpass filter; D_i, avalanche photodiode; G, transmission grating; LPF, long-pass filter; CL, cylindrical lens.

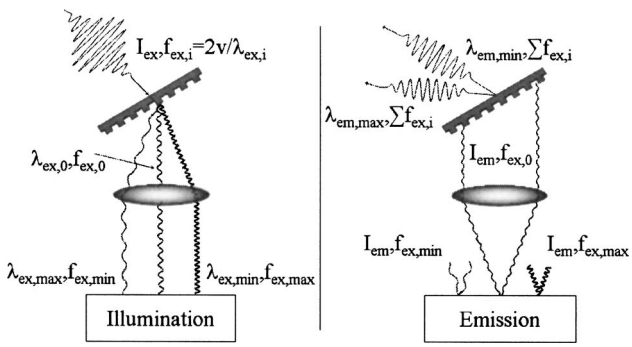

Fig. 2. SFE fluorescence imaging concept: I_{ex}, illumination spectrum; f, modulation frequency of the light; v, mirror velocity; I_{em}, fluorescence emission spectrum.

whose intensity was

$$I_{ex}(\lambda_{ex,i},t) = \frac{1}{2} I_{ex}(\lambda_{ex,i}) \left[1 + \cos\left(\frac{4\pi}{\lambda_{ex,i}} vt \right) \right], \qquad (2)$$

where $I_{ex}(\lambda_{ex,i})$ is the spectral intensity corresponding to the ith wavelength ($\lambda_{ex,i}$) of the excitation light and v is the velocity of the interferometer scanning mirror. As long as the interferometer scans a large enough distance to provide sufficient spectral resolution, the number of resolvable points in SFE fluorescence imaging is also governed by Eq. (1).

A compact grating–lens pair was used to illuminate the sample, simulating a ~1 mm diameter miniature endoscope. The lens (f=12.5 mm) focused each of the uniquely modulated excitation wavelengths onto a different location of the sample after they had been dispersed by the holographic transmission grating (G, 1200 lines/mm, Fig. 2, left). The fluorescence emission at each location was consequently modulated at the frequency $f_{ex,i}=2v/\lambda_{ex,i}$ (Fig. 2, right; I_{em} is the entire fluorescence emission spectrum). Light from a helium–neon laser was also directed through the interferometer and deflected through a 633 nm bandpass filter (BPF, Fig. 1) for detection by an avalanche photodiode (D_R, Hamamatsu C5460) to obtain a reference signal for correction of scanning mirror nonlinearities.

Emitted light was transmitted back through the same lens and grating. The fluorescence, which was diffracted at a different angle than the reflected light, was then deflected by a mirror (Fig. 1) through an 830 nm long-pass filter (LPF) and focused onto a second avalanche photodiode (D_F,) by a combination of spherical and cylindrical lenses (CL). In this particular configuration the grating was mounted to a galvanometer and rotated to provide the slow-axis scanning. Reconstruction of the image was accomplished by taking the Fourier transform of the modulated fluorescence for each galvanometer scan angle after using the reference signal to correct the interferogram.

Indocyanine green (ICG) is a near-infrared fluorophore (excitation 650–850 nm, emission 805–950 nm) that has been approved by the Federal Drug Administration for several clinical indications[7] and has been modified for targeted antibody labeling.[8,9] Figure 3a shows a fluorescence image of microfluidic channels[10] filled with ICG (2 mg ICG/ml dimethyl sulfoxide, DMSO) obtained by using the SFE technique. Note the presence of an air bubble in the middle of the rightmost vertical channel in the fluorescence image. A corresponding epiilluminated reflectance micrograph is shown in Fig. 3b, clearly demarcating the smallest, 35 μm wide channels. The SFE image was collected at 2 Hz with a 1.4 mm × 1.4 mm field of view. The center wavelength and the spectral range (full width at 15% maximum) of illumination after low-pass filtering were 780 and 50 nm, respectively. The Michelson interferometer scanning mirror was translated ±0.25 mm around the zero-path-length difference position to provide a spectral resolution of ~0.6 nm, corresponding to a theoretical 83 resolvable points, or 16.9 μm spatial resolution across the 1.4 mm field of view.[11] The probe input beam was 1.1 mm in diameter and was incident on the grating at 22°, also resulting in a spectral resolution of 0.6 nm and 83 resolvable points. Since the usable excitation bandwidth of ICG is 125 nm in DMSO, this probe configuration could theoretically enable >200 resolvable points per frequency-encoded line, providing

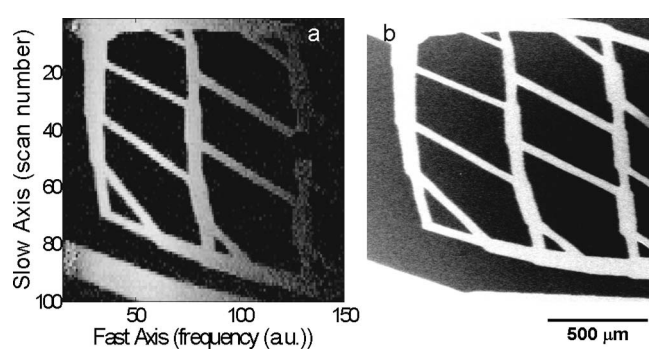

Fig. 3. Images of microfluidic channels: a, ICG fluorescence in channels imaged with SFE and b, white-light microscope image of similar channels. Scale bar, 500 μm.

Table 1. Theoretical Number of SFE Resolvable Points for Typical Fluorophores[a]

Fluorophore	Excitation Bandwidth (nm)	Points for Beam Diameter	
		1.0 mm	0.5 mm
GFP	145 (375–520)	266,000	66,000
FITC	90 (430–520)	92,000	23,000
Cy5.5	110 (570–680)	89,000	22,000
ICG (plasma)	184 (670–854)	195,000	49,000

[a]Number of points for beam diameter rounded to nearest fourth digit. SFE parameters; 1500 lines/nm grating, incident illumination at Littrow's angle. The excitation bandwidth is defined as the full width at 10% maximum.

resolution greater than 7 μm. However, the limited bandwidth of the current source reduced this number to 84, resulting in a resolution of 16.7 μm.

Lateral resolution measurements along the spectrally encoded line were estimated by measuring the edge response function of 15 lines in the image along the wavelength-encoded axis at vertical edges in the microfluidic channels. Our measurements demonstrated a spatial resolution of 15.9 ± 4.9 μm (mean $\pm$ standard deviation), corresponding to a total of approximately 88 resolvable points across the field of view, which was in agreement with the theoretical calculation. Resolution along the transverse axis was theoretically limited to 10.8 μm by the imaging optics; however, the actual resolution was set at 14 μm by the scanning rate to roughly match the lateral resolution.

The total number of resolvable points obtained by our SFE fluorescence imaging apparatus, which approximated the dimensions of a 1 mm endoscope, is $n^2 = 7{,}744$. This value is comparable with state-of-the-art fiber-bundle-based technologies of similar diameter and can be easily improved by increasing the excitation bandwidth or utilizing a higher-density grating while simultaneously increasing the scanning range of the interferometer.

For a given beam diameter, the number of resolvable points attained by SFE is affected by the excitation spectra of the fluorophores. Table 1 depicts the predicted number of resolvable points for several common fluorescent labels, assuming beam diameters of 1.0 and 0.5 mm and a grating groove density of 1500 lines/mm. For each case, the theoretical number of resolvable points either equals or exceeds that of fiber bundles with comparable diameters. In order to attain this performance, the source must be capable of illuminating the entire excitation spectrum, which is now possible with photonic crystal fiber technology and supercontinuum generation.[12]

Since SFE may be conducted with a single optical fiber, images obtained by this technique do not contain pixelation artifacts that are commonly observed in fiber bundles.[1] Furthermore, the flexibility of the SFE miniature probe will be greatly increased, as the bend radius for a single fiber is significantly less than that of imaging bundles. These advantages of SFE could be of significant benefit for applications where image quality and maneuverability are of concern.

In order to minimize size in the development of future SFE endoscopes, it may be advantageous to collect the fluorescent emission through the probe grating. Stokes-shifted fluorescent light, however, will not couple back to the core of a single-mode illumination fiber. An attractive solution to this challenge may be the use of a dual-clad fiber[13] such that excitation light is transmitted through the central core and the fluorescence is gathered through the inner cladding. Using ray-tracing models, we have investigated this approach and have found that it may work without significantly increasing the probe diameter or compromising resolution.

In conclusion, we have demonstrated a novel technique, spectral- and frequency-encoded fluorescence imaging, with a clinically approved near-infrared fluorochrome. Further development of this technology may enable fluorescent imaging through flexible miniature endoscopes.

The authors thank Eli Weinberg and Jeffrey Borenstein for providing the microfluidic channels and Johannes de Boer and his group for use of the laser. This research was supported by the Whitaker Foundation (grant RG-01-0392), the Medical Free Electron Laser program funded by the Air Force Office of Scientific Research, Department of Defense (award FA9550-04-1-0079), and the National Institutes of Health (grant 5 T32 AR07098; T.S. Kupper, Principal Investigator). J. T. Motz's e-mail address is jmotz@partners.org.

References

1. E. Laemmel, M. Genet, G. Le Goualher, A. Perchant, J. F. Le Gargasson, and E. Vicaut, J. Vasc. Res. **41**, 400 (2004).
2. M. A. Funovics, H. Alencar, H. S. Su, K. Khashayarsha, R. Weissleder, and U. Mahmood, Molecular Imaging **2**, 350 (2003).
3. M. A. Funovics, R. Weissleder, and U. Mahmood, Radiology **231**, 659 (2004).
4. G. J. Tearney, R. H. Webb, and B. E. Bouma, Opt. Lett. **23**, 1152 (1998).
5. G. J. Tearney, M. Shishkov, and B. E. Bouma, Opt. Lett. **27**, 412 (2002).
6. G. J. Tearney, S. A. Boppart, B. E. Bouma, M. E. Brezinski, N. J. Weissman, J. F. Southern, and J. G. Fujimoto, Opt. Lett. **21**, 543 (1996).
7. C. H. Tung, Biopolymers **76**, 391 (2004).
8. S. Ito, N. Muguruma, Y. Kusaka, M. Tadatsu, K. Inayama, Y. Musashi, M. Yano, T. Bando, H. Honda, I. Shimizu, K. Li, K. Takesako, H. Takeuchi, and S. Shibamura, Endoscopy **33**, 849 (2001).
9. T. Bando, N. Muguruma, S. Ito, Y. Musashi, K. Inayama, Y. Kusaka, M. Tadatsu, K. Ii, T. Irimura, S. Shibamura, and K. Takesakos, Gastroenterol. J. **37**(4), 260 (2002).
10. M. Shin, K. Matsuda, O. Ishii, H. Terai, M. Kaazempur-Mofrad, J. Borenstein, M. Detmar, and J. P. Vacanti, Biomed. Microdevices **6**, 269 (2004).
11. J. Kauppinen and J. Partanen, *Fourier Transforms in Spectroscopy* (Wiley-VCH, 2001), p. 271.
12. G. McConnell, Opt. Express **12**, 2844 (2004).
13. D. Yelin, B. E. Bouma, S. H. Yun, and G. J. Tearney, Opt. Lett. **29**, 2408 (2004).